Title: Safe and fast-charging Li-ion battery with long shelf life for power applications

Authors: K. Zaghib, M. Dontigny, A. Guerfi, P. Charest, I. Rodrigues, A. Mauger, C.M. Julien

PII: S0378-7753(10)02084-7
DOI: doi:10.1016/j.jpowsour.2010.11.093
Reference: POWER 13873

To appear in: *Journal of Power Sources*

Received date: 30-9-2010
Revised date: 12-11-2010
Accepted date: 17-11-2010

Please cite this article as: K. Zaghib, M. Dontigny, A. Guerfi, P. Charest, I. Rodrigues, A. Mauger, C.M. Julien, Safe and fast-charging Li-ion battery with long shelf life for power applications, *Journal of Power Sources* (2010), doi:10.1016/j.jpowsour.2010.11.093

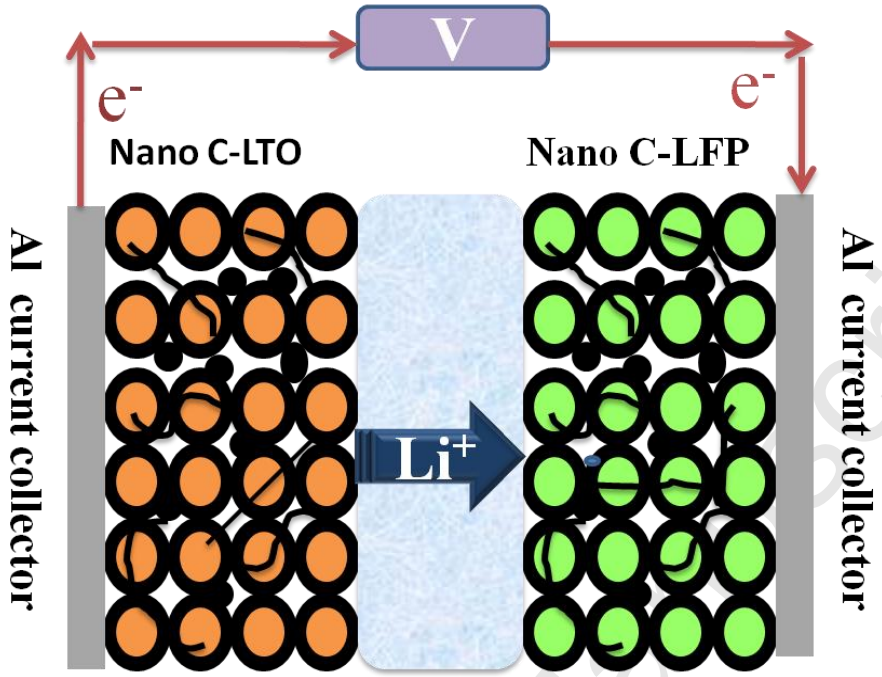

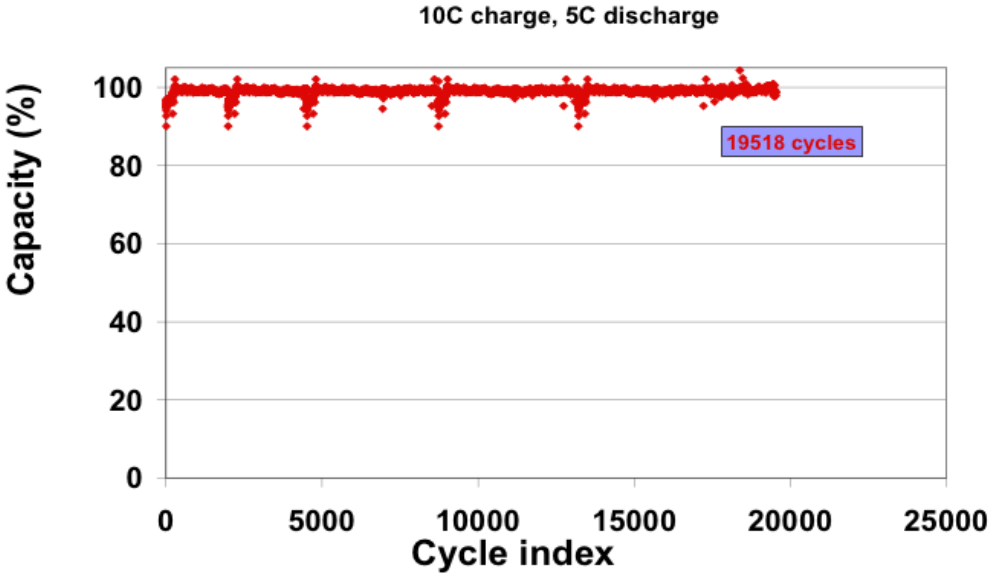

Safe and fast-charging Li-ion battery with long shelf life for power applications

K.Zaghib,[1] M. Dontigny[1], A. Guerfi[1], P. Charest[1], I. Rodrigues[1], A. Mauger[2], C.M. Julien[3]

[1]Institut de Recherche d'Hydro-Québec, Varennes, QC, Canada J3X 1S1

[2]Institut de Minéralogie et de Physique des Milieux Condensés, Université Pierre et Marie Curie, 140 rue de Lourmel, 75015 Paris, France.

[3]Laboratoire de Physicochimie des Electrolytes, Colloïdes et Sciences Analytiques, Université Pierre et Marie Curie, Bat. F, 4 place Jussieu, 75005 Paris, France.

Abstract

We report a Li-ion battery that can be charged within few minutes, passes the safety tests, and has a very long shelf life. The active materials are nanoparticles of $LiFePO_4$ (LFP) and $Li_4Ti_5O_{12}$ (LTO) for the positive and negative electrodes, respectively. The $LiFePO_4$ particles are covered with 2 wt.% carbon to optimize the electrical conductivity, but not the $Li_4Ti_5O_{12}$ particles. The electrolyte is the usual carbonate solvent. The binder is a water-soluble elastomer. The "18650" battery prepared under such conditions delivers a capacity of 800 mAh. It retains full capacity after 20,000 cycles performed at charge rate 10C (6 min), discharge rate 5C (12 min), and retains 95% capacity after 30,000 cycles at charge rate 15C (4 mn) and discharge rate 5C both at 100 % DOD and 100 % SOC.

Keywords: Li-ion batteries, olivines, titanates.

1. Introduction

Global warming, finite fossil-fuel supplies, and pollution make the replacement of petroleum with electric propulsion an imperative across the world. Li-ion batteries are expected to power the next generation of electric vehicles (EVs). However, performance, service life, and most important, safety, are issues that continue to plague the development of the Li battery for the mass market of EVs to alleviate distributed CO_2 emissions and noise pollution. We report in this work a battery that fulfills these requirements. To reach this goal, the different elements of the cell have been optimized. The costly and toxic $LiCoO_2$ active element of the positive electrode has been replaced by the cheaper and environment friendly $LiFePO_4$ (LFP) coated with 2 wt.% conductive carbon [1-2]. High power requires small sizes for the particles, but nanoparticles are difficult to handle and reduce the tap density [3], so that we used particles of size 25 nm considered as the best compromise.

The standard anode of the Li-batteries is carbon based. However, carbon requires formation of a solid/electrolyte-interface (SEI) to prevent the formation plating of Li on the carbon anode during a fast charge of the battery, and the SEI layer is responsible of an irreversible capacity loss. Instead, we used $Li_4Ti_5O_{12}$ (LTO). This spinel structure has been proposed as a promising candidate [4] as a negative electrode with different positive electrodes, including $LiFePO_4$ [5]. The electro-activity occurs at a voltage higher than 1.0 V. Therefore, the electrode does not experience the passivation of the anode materials and their inevitable electrolyte reaction. Also the lack of strain in this material improves the shelf life, and is another improvement with respect to the carbon that suffers dilatation/contraction upon insertion/extraction of lithium resulting in aging.

Power applications require an electrolyte with high ionic conductivity $\sigma > 10^{-3}$ S/cm [6], so we kept the most commonly used blend consisting of ethylene carbonate (EC) and diethyl carbonate (DEC).

The binder material is also one of the crucial components for improved cell performance. We have used an elastomer instead of the traditional PVdF binder for the positive electrode, since it permits a high active material ratio in the electrode and more elasticity between particles. Furthermore, the electrode composition is prepared in aqueous solution, which gives to another economic and environmental advantage.

The LFP/LTO cell has passed successfully the required battery tests for safety use in transportation. The aging is negligible over thousands of cycles even at high C-rate. It would take an equivalent of 50 years to achieve this number of cycles if one cycle is performed per day. It is thus an important jump in the technology since, for the first time, the shelf life is not

limited by the use of the battery, but by the stability of its components. In practice, it means that a battery made with such cells to power an electric car will be guaranteed for the life of the car, a performance that is expected to boost this market.

2. Experimental

In the first step, $LiFePO_4$ has been synthesized according to the procedure described in [7]. An excess of 0.5 mole-fraction of EBN-1010 (graphite powder) was added to the initial product as a reducing agent for iron by carbothermal effect. Then, the mixture has been heated to 1050 °C during 5 mn and then cooled under N_2. The ingot obtained by this way is a rock of typical size 10 cm. Next steps for reducing the size of the particles are the use a jaw-crusher with ceramic liner to avoid metal contamination, then a roll crusher (ceramic type), they jet-mill to decrease the size to cm, mm, μm, respectively. In the wet-milling process, the μm-sized powder is then dispersed in isopropyl alcohol (IPA) solution at 10-15% of solid concentration and ground on a bead mill using 0.2 mm zirconia's beads to obtain nanometer-sized particles [8].

The second step was to coat the particles with carbon. For this purpose, the particles were mixed with the carbon precursor (lactose) in aqueous solution. The dry additive corresponded to ~5 wt.% of the carbon source in $LiFePO_4$. After drying, the blend was heated at 700 °C for 4h under neutral atmosphere. The residual carbon in the final product represents about 2 wt% of the material (measured with C-detector, LECO Co., CS 444).

$Li_4Ti_5O_{12}$ was prepared by solid-state reaction of precursor materials TiO_2, Li_2CO_3 and carbon heated at 850 °C during 18 h, according to a synthesis procedure detailed in Refs. [9-10].

The binder used for the $LiFePO_4$ particles is water-soluble. It is an elastomer based on saturated organic compounds obtained from ZEON Corp., Japan. The thickener is sodium carboxymethyl cellulose (CMC) (Daicel 2200, Daicel Chemical Industries Ltd., Japan), styrene-butadiene rubber (SBR) is the primary water soluble binder (WSB). A slurry consisting of 90 wt.% of $LiFePO_4$, 6 wt.% carbon black, 2 wt.% CMC and 2 wt.% WSB by using water solvent was prepared by ball-milling. Mixing the slurry is very important to get a better dispersion of powders material in the polymer matrix and more uniform electrodes. The well-dispersed slurry between conducting carbon and CMC provides very uniform dispersion and uniform contact with $LiFePO_4$ particles. The polymer (binder and CMC) ratio was adjusted to improve the adhesion of the particles to the current collector.

The crystal structure of the particles was analyzed by X-ray diffraction (XRD). The XRD pattern of the $LiFePO_4$ and the $Li_4Ti_5O_{12}$ particles are well known and not reported here. The patterns are found to be those of the pure materials. Due to the very poor sensitivity of the XRD analysis, we have also characterized the materials by other techniques: infrared spectroscopy and magnetic measurements. We refer to our prior works (see for instance Ref. [11]) for the details of the apparatus we have used for this purpose, and for the analysis of the data. As a result, no impurity has been detected for the powders used in this work.

Scanning electron (SEM) and transmission electron microscopy (TEM) images were obtained using an electronic microscope Hitachi model HD-2700 with 200 kV, 120 kV and 80 kV operating potential.

3. Results

3.1. Positive electrode

The positive electrode is the key element that determines the safety and performance of the Li-batteries. The winning element at present time is $LiFePO_4$ for power batteries to be used for transportation applications where the safety issues are crucial, because it is the only positive electrode so far that can pass all of the safety tests, namely nail and rod penetration test and short-circuit tests. Many synthesis routes have been adopted to produce $LiFePO_4$ material, which have been reviewed elsewhere [12]. Nowadays, most processes can be used to obtain $LiFePO_4$ powder with capacity close to theoretical, provided the synthesis is performed under reducing atmosphere to avoid the oxidation of iron resulting in Fe^{3+}-based impurity phases [11]. However, another parameter greatly influences the rate capability, namely the particle size, and it is then important to monitor it. For this purpose, synthesis of $LiFePO_4$ in the molten state has been proposed [13]. We have shown recently that it offers the desired flexibility to choose the size of the particles in the whole range from macroscopic to nanometer size by milling processes. For applications that require power, small particles are needed, because the diffusion of Li in $LiFePO_4$ is small so that the pathway of the travel of the Li^+ ions should be minimized. On another hand, too small particles have been reported to decrease the tap density [14]; so, in this work we have chosen particles of average size 25 nm, which is estimated to be the best compromise. In addition, Li^+ ions preferably move along the *b*-axis of the crystal with orthorhombic space group *Pnma* [15-16]. It is then desirable to reduce the crystallite size along this axis. This is, however, a difficult problem, because, there is a tendency of the particles to grow under the form of plates in the (*ab*) plane [17-18]. Another advantage of the preparation from the molten state is the more spherical shape of the

particles. Another advantage is that the particles that are obtained in this process are well crystallized, while $LiFePO_4$ particles to such a small size obtained by other process are often ill-crystallized, and contain a large concentration of defects that are detrimental to the electrochemical properties [19].

On another hand, the particles after milling need carbon-coating to increase the electronic conductivity. This amount of carbon deposited (2 wt% of the final product) is chosen on purpose as a compromise. Since the charge rate that is supported by the battery increases with the amount of carbon, graphitization degree and its adhesion on the surface of LFP particles, the tests in laboratory tend to be performed with larger amounts of carbon to get better performance. For instance, first discharge rate of 105 mAh/g at 20C-rate and 75 mAh/g at 60 C-rate has been reported for $LiFePO_4$ particles with 20 wt.% acetylene black [20]. An extreme case is 65 wt.% carbon to reach ultra-fast C-rate [21], a result that has been criticized [22]. However, in Li-ion batteries for commercial use, the amount of carbon must be small, say $\leq$ 5 wt.%, because carbon is an inert mass, and also because larger amounts of carbon lead to the formation of carbon powder between the particles instead of a coating (nano-painting) of the particles with carbon, resulting in aging. We have then chosen the amount of carbon that corresponds to a realistic Li-ion battery for commercial use.

The carbon coating at 700 °C has another positive effect on the surface layer of the particles. Before carbon coating, the surface layer is severely disordered, which can be detrimental to the electrochemical properties. The heating process cures this disorder; it is partly due to the Fe-C interaction [23]. It is also partly due to re-crystallization of the surface layer upon heating. Indeed, our infrared spectroscopy measurements show a shrinking of the absorption peaks associated to the vibration modes upon heating the uncoated particles without carbon additive [12]. The shrinking is the signature of a longer lifetime of the phonons and gives evidence of reduced disorder effects. Actually, the conductivity of the carbon coat increases with the temperature [24]. On another hand, heating above 750 °C results in an inter-diffusion between particles so that individual particles tend to coalesce. We have then identified 700 °C as the optimum temperature. The result is a $LiFePO_4$ powder with particle size ca. 25 nm, which is comparable with the size of the coherence length deduced from the X-ray diffraction (XRD) pattern by applying the Scherrer law. The size of the particles measured from a laser diffraction analyzer is about 100 nm, which shows a slight agglomeration of the particles. On one hand, the small size of the primary particles optimizes the electrochemical performance, while the size of the secondary particles is best suited to the handling of the powder, as mentioned in the previous section. The SEM and TEM images of

the powder are illustrated in Fig. 1. Note that the primary particles have still a uniform carbon coverage despite aggregation to secondary particles.

3.2. Negative electrode

The standard anode used for Li-ion batteries is graphite. However, the formation of a passivation layer at the surface of graphite inevitably generates an internal resistance and decreases the performance of the battery. Therefore, we have chosen $Li_4Ti_5O_{12}$ as the active element of the anode, since it avoids the formation of any SEI layer and the very small dilatation/contraction of the lattice upon lithiation/delithiation makes possible the use of fast cycling without any damage to the particles. It is now possible to prepare $Li_4Ti_5O_{12}$ by different synthesis processes [25]. We have adopted a route that allows us to obtain nanoparticles [26], with high capacity retention: 160 mAh/g at 5C. The secondary particles are crystallites. Their average size deduced from the Scherrer formula and the electron microscope images is 150 nm. The XRD pattern is also used to check the absence of the peaks associated to TiO_2, TiO, and Li_2TiO_3 impurities that are observed when the synthesis temperature is smaller than 800 °C. The high resolution TEM in Fig. 2 shows particles that are crystallized without any defect, before the wet milling that reduces their size to 150 nm. It shows that the surface layer is less disordered than that of $LiFePO_4$, but over a thickness that is about the same, the order of 3 nm. Note that the LTO particles are not carbon coated.

3.3. Electrolyte

For power batteries, the choice among all of the electrolytes that have been envisioned so far is limited to organic liquids [6], taking into account the fact that inorganic solid electrolytes can be used only in thin-film battery applications. We have then kept the reference commercial electrolyte EC/DEC-1*M* $LiPF_6$ that is extensively used, due to its high conductivity $\sigma = 7\times10^{-3}$ S/cm. $LiPF_6$ is also the preferred salt in the Li-ion batteries, because it avoids the formation of a SEI at the surface of the aluminum current collector.

3.4. Binder

The poly(vinylidene fluoride) (PVdF) product has been most widely adopted as a binder for electrodes in Li-ion batteries. It has strong binding strength, but its low flexibility can easily deteriorate cycle life of the battery due to the breaking of the bond between the active particles upon their dilatation/contraction during lithiation/delithiation. To absorb these stresses, and improve the shelf life, it is necessary to choose a binder having elasticity. In

addition, a binder such as PVdF that is soluble only in a solvent is dangerous to humans and the environment. The switch from non-aqueous to aqueous binders is thus imperative [7]. It has the following advantages: low cost, no pollution problem, reduction of the binder content, fast drying. Recently, aqueous binders have been commercially used for the anode, but not yet for the positive electrode. Here, we used a new water-soluble binder that we have successfully tested with $LiFePO_4$, which leads to lower irreversible capacity losses.

3.5. Electrochemical performance

The electrochemical performance of the $LiFePO_4$ and $Li_4Ti_5O_{12}$ materials has been tested separately in half cell with respect to Li metal anode, using the same electrolyte mentioned above. The voltage *vs.* capacity curves recorded under such conditions at 25 °C are reported in Fig. 3 at low C-rate C/24 to approach thermodynamic equilibrium together with the potential-capacity curve of the LTO//LFP lithium-ion battery. The voltage window is 2-4 V for $LiFePO_4$, 1.2-2.5 V for $Li_4Ti_5O_{12}$. Note in this figure (and the following ones), we have kept the conventional rule, i.e. the capacity is in mAh per gram of the active element of the cathode. That is the reason why the maximum capacity for the $LiFePO_4$//Li and $LiFePO_4$// $Li_4Ti_5O_{12}$ are the same. For $LiFePO_4$//Li, the first coulombic efficiency is 100 % and the reversible capacity is 148 mAh/g. For $Li_4Ti_5O_{12}$, the first coulombic efficiency is 98% and the reversible capacity is 157 mAh/g. The well-known plateaus at 3.4 and 1.55 V are characteristics of the topotactic insertion/deinsertion of lithium in the two-phase systems $LiFePO_4$-$FePO_4$ and $Li_4Ti_5O_{12}$-$Li_7Ti_5O_{12}$, respectively. The Ragone plots in Fig. 4 show that the high rate capacity of both materials is stable up to 5C. At 10C, $LiFePO_4$ still delivers 73% of the rated capacity against 53% for $Li_4Ti_5O_{12}$. The $LiFePO_4$/EC-DEC-1*M* $LiPF_6$/ $Li_4Ti_5O_{12}$ batteries '18650' have been made with these products.

Plots of galvanostatic charge-discharge curves at different cycles, i.e. 1st, 10,000th, 20,000th and 30,000th, for both 10C charge rate and 15C charge rate are shown in Figs. 5 and 6, respectively. To complement the electrochemical performance of the LFP//LTO 18650-batteries, the cycling life is illustrated in Fig. 7 for charge rate at 10C (6 mn) and discharge rate 5C (12 mn). Even after 20,000 cycles, the cell did not loose its initial capacity. The voltage-capacity curves for the LTO//LFP cell during the test (Fig. 5) are showing very little difference, even at the end of the test. The cycling life of another cell is illustrated in Fig. 8 over 30,000 cycles for faster charge rate at 15C (4 mn), and the same discharge rate at 5C that correspond to the plots of galvanostatic charge-discharge curves shown in are reported in Fig. 6 at different cycle numbers. For this case, the capacity (910 mAh in the first cycles)

decreases with the number of cycles, but the loss at the end of the process is only 9%, which can be considered as negligible based on one charge-discharge cycle each day (a rather intense use for portable applications) would take 50 years of life. Note that full depth of discharge (DOD) has been achieved for each cycle in all these experiments. This is to our knowledge a breakthrough in the performance of Li-ion batteries since their poor cycling life was considered as a major defect.

During the transportation tests performed on these batteries, no flame and no smoke have been detected, and the maximum temperature that has been reached is 72 °C. For comparison, in the same tests, the $LiCoO_2$//graphite 18650-cell goes on fire with heavy smoke, the temperature reaching 350 °C. $LiMn_2O_4$//graphite cells also go on fire in the short circuit test.

4. Discussion

These results show that LFP//LTO Li-ion cells are safe and can support fast charge/discharge rates without any damage for the cycling life. The impact on electric cars will be important, since it is the most demanding use in terms of performance and safety. The fast charge and discharge rates tested in this work are typically needed upon driving to accelerate (discharge) or slow (recharge) the car. It also means that the use of a battery in a car cannot be mimicked simply by periodic cycles like in the classical procedure we have followed to test batteries. The time spend in acceleration and deceleration during the number of kilometers or miles before the battery is discharged may be typically 50 mn, while the time spent to reach 100% DOD during one cycle tested in the present work is typically 10 minutes. But even then, the cycling life investigated in the present work means that this battery can survive with negligible lost for more than 5 years, a typical life for a vehicle. Other parameters that are out of reach in the test performed in the laboratory is the decomposition of the electrolyte that shortens the life of the battery at high temperature, in particular that of $LiPF_6$. This preferred salt can undergo an autocatalytic decomposition into LiF and PF_5. This reaction degrades the battery. However, additives used to lower the operating temperature also prevent this decomposition [26].

The price to be paid for the substitution of the carbon anode by $Li_4Ti_5O_{12}$ is a loss of energy density that decreases from approximately from 100 to 67.5 Wh/kg, due to the lower operating voltage of the cell resulting form the LTO plateau at 1.55 V as shown in Fig. 3. Today, the most performing electric commercialized car is equipped with $LiFePO_4$/graphite cells that allows for a driving range of about 300 km, which would be reduced to 200 km

when equipped with the batteries investigated in the present work. It is still more then needed for many daily uses, and we consider that this inconvenience is worth the safety and long shelf life gained in the process. Moreover, a fully discharged battery of an electric car with driving range of 300 km cannot be recharged in 5 minutes, because the electric grid cannot supply the power needed to charge a battery of energy ranging between 15 and 50 kWh in 5 minutes [22] at a reasonable cost. On another hand, this performance becomes possible for a city car. This technology is under demonstration at Hydroquébec and is illustrated in figure 9; the car equipped with the battery built with the LFP//LTO cells described in the present work weights 680 kg, has a driving range of 32 km (50 km optional), with top speed 64 km/h. The battery capacity is 2.9 kWh only, which makes possible the full charge in 5 minutes by using parallel charger with 380 V plug-in.

We have shown [23] that it is possible to coat the $Li_4Ti_5O_{12}$ particles with carbon to reach a conductivity of $\sigma = 4\times10^{-4}$ S/cm. However, the cell presented in this work has been made with uncoated $Li_4Ti_5O_{12}$ particles, which reduces the cost and proves that the coating is not mandatory for these particles even to reach the performance shown in this work.

The long cycling life that has been reached implies that more attention should now be focused on the improvement of other elements of the battery, in particular the electrolyte and lithium salt as mentioned before. The use of ionic liquids is under investigation. More stable salts, LiTFSI or LiFSI, can replace the reference salt $LiPF_6$, where FSI and TFSI stand for bis- and tri-(fluorosulfo-nyl)imide, respectively. LiTFSI corrodes aluminum, but the first experiences with LiFSI are very promising [27]. In particular, the capacity of a cell with LiFSI starts diverging from the cell with $LiPF_6$ only above 20C rate. On another hand, it is not yet possible to get rid of the organic solvent of the electrolyte. The best that be done is to decrease its proportion by substituting about 30 mol.% of ionic liquid to save the performance of the battery [28]. We then expect that some improvements will still occur in the next years to come.

5. Conclusion

The Li-ion battery presented in this work has filled a gap in the performance in terms of safety, cycling life, which are key-issues in public transportation. It opens the route to the construction of city EVs equipped with Li-ion batteries that will not need to be changed, and can be charged in 5 mn. It thus opens new routes to the energy storage of post-oil industry, but it also questions whether a “reasonable” use of the Li-ion batteries should not be limited to transportation at the scale of a city car. Finally, to highlight the use of the most advanced

Li-ion batteries, we show (Fig. 9) cars presented at the World Energy Council (Montréal, Sept. 2010), equipped with the battery C-LFP/LTO built with the same cells as described in the present work. Charging time is reduced to 5 minutes with three levels charger in parallel (500 V, 125 A).

Acknowledgment

The authors are grateful to Dr. Donald N.H. Wu from PHET for the fabrication of EVs by using an innovative DOSBAS® battery system for electric vehicles based upon lithium iron phosphates chemistry.

References

1. A.K. Padhi, K.S. Nanjundaswamy, J.B. Goodenough, J. Electrochem. Soc. 144 (1997) 1188.
2. N. Ravet, Y. Chouinard, J. F. Magnan, S. Besner, M. Gauthier, M. Armand, J. Power Sources 97 (2001) 503.
3. Z.H. Chen J.R. Dahn, J. Electrochem. Soc. 149 (2002) A1184.
4. N. Ravet, Y. Chouinard, J.F. Magnan, S. Besner, M. Gauthier, M. Armand, J. Power Sources 97-98 (2003) 503.
5. N. Ohta, T. Sogabe, K. Kuroda, Carbon 39 (2001) 1434.
6. J. B. Goodenough, Y. Kim, Chem. Mater. 22 (2010) 587.
7. A. Guerfi, M. Kaneko, M. Petitclerc, M. Mori, K. Zaghib, J. Power Sources 163 (2007) 1047.
8. G. Luang, P. Charest, C. Michot, A. Guerfi, M. Gauthier, K. Zaghib, Patent WO 2008/0676677 A1.
9. A. Guerfi, S. Sévigny, M. Lagacé, P. Hovington, K. Kinoshita, K. Zaghib, J. Power Sources 119-121 (2003) 88.
10. A. Guerfi, P. Charest, K. Kinoshita, M. Perrier, K. Zaghib, J. Power Sources 126 (2004) 163.
11. A. Ait-Salah, A. Mauger, C. M. Julien, F. Gendron, Mater. Sci. Eng. B 129 (2006) 232.
12. K. Zaghib, P. Charest, M. Dontigny, J.F. Labrecque, A. Mauger, F. Gendron, C.M. Julien, J. Power Sources, in press.
13. K. Zaghib, G. Liang, J. Labrecque, A. Mauger, C.M. Julien, Abs. n° 582, PRIME 2008 Meeting, Honolulu (USA).
14. Z.H. Chen, J.R. Dahn, J. Electrochem. Soc. 149 (2002) A1184.
15. T. Maxisch, F. Zhou, G. Ceder, Phys. Rev. B 73 (2006) 104301.
16. M. S. Islam, D. J. Driscoll, C. A. Fischer, P. R. Slater, Chem. Mater. 17 (2005) 5085.
17. G. Chen, X. Song, T. J. Richardson, J. Electrochem. Soc. 154 (2007) A627.
18. T. J. Richardson, 3rd Annual Conference - LITHIUM MOBILE POWER 2007 - Advances in Lithium Battery Technologies for Mobile Applications (San Diego, USA).
19. L. Laffont, C. Delacourt, P. Gibot, M. Yue Wu, P. Kooyman, C. Masquelier, J. M. Tarascon, Chem. Mater. 18 (2006) 5520.

20. M. Konarova, I. Taniguchi, J. Power Sources 195 (2010) 3661.
21. B. Kang, G. Ceder, Nature 458 (2009) 190.
22. K. Zaghib, J. B. Goodenough, A. Mauger, C.M. Julien, J. Power Sources 194 (2009) 1021.
23. K. Zaghib, A. Mauger, F. Gendron, C.M. Julien, Chem. Mater. 20 (2008) 462.
24. C.M. Julien, K. Zaghib, A. Mauger, M. Massot, Ait-Salah, M. Selmane, F. Gendron, J. Appl. Phys. 100 (2006) 63511.
25. A. S. Prakash, P. Manikandan, K. Ramesha, M. Sathiya, J.-M. Tarascon, A.K. Shukla, Chem. Mater. in press, DOI:10.1021/cm10071z.
26. M.C. Smart, K.A. Smith, R.V. Bugga, L.D. Whitcanack, in Electrolytes for Wide Operating Temperature Range Li-ion Cells, 4th Annual Conference: Lithium Mobile Power 2008, Las Vegas, NV, 2008.
27. See for instance A. Guerfi, S. Duchesne, Y. Kobayashi, A. Vijh, K. Zaghib, J. Power Sources 175 (2008) 866.
28. A. Guerfi, M. Dontigny, P. Charest, M. Petitclerc, M. Lagacé, A. Vijh, K. Zaghib, J. Power Sources 195 (2010) 845.

Figure captions

Fig. 1. Transmission electron microscope images of $LiFePO_4$ particles after carbon-coating.

Fig. 2. Transmission electron microscope images of $Li_4Ti_5O_{12}$ particles. Note that LTO particles were not carbon-coated.

Fig. 3. Voltage-capacity cycle for $LiFePO_4$/EC-DEC-1*M* $LiPF_6$/Li, $Li_4Ti_5O_{12}$/EC-DEC-1*M* $LiPF_6$/Li, and $LiFePO_4$/EC-DEC-1*M* $LiPF_6$/$Li_4Ti_5O_{12}$ at C/24 rate. The capacity is in mAh per gram of the positive electrode element ($LiFePO_4$, $Li_4Ti_5O_{12}$, $LiFePO_4$, respectively). The larger hysteresis in the $LiFePO_4$/EC-DEC-1*M* $LiPF_6$/$Li_4Ti_5O_{12}$ cell comes from the fact that the cell in that case was a button cell instead of the more elaborate 18650-cell, but the plateau at 1.9 V is well observed. The voltage-capacity cycles for the 18650-cells are reported in next figures

Fig. 4. Ragone plots of the $LiFePO_4$/EC-DEC-1*M* $LiPF_6$/Li and $Li_4Ti_5O_{12}$/EC-DEC-1*M* $LiPF_6$/Li 18650-cells.

Fig. 5. Voltage-capacity cycles of the $LiFePO_4$/EC-DEC-1*M* $LiPF_6$/$Li_4Ti_5O_{12}$ (cycle charge rate is 10C, the discharge rate is 5C. The spikes are due to computer buffer saturation and the creation of new files because the great number of data.

Fig. 6. Voltage-capacity cycles of the $LiFePO_4$/EC-DEC-1*M* $LiPF_6$/$Li_4Ti_5O_{12}$ (cycle charge rate is 15C, the discharge rate is 5C). The spikes are due to computer buffer saturation and the creation of new files because the great number of data.

Fig. 7. Cycle life of a $LiFePO_4$/EC-DEC-1*M* $LiPF_6$/$Li_4Ti_5O_{12}$ 18650-cell. The cycle charge rate is 10C (6 min) at 100 % SOC, the discharge rate is 5C (12 min) at 100 % DOD during the test reported in Fig. 5.

Fig. 8. Cycle life of a $LiFePO_4$/EC-DEC-1*M* $LiPF_6$/$Li_4Ti_5O_{12}$ 18650-cell. The cycle charge rate is 15C (4 min) at 100 % SOC, the discharge rate is 5C (12 min) at 100 % DOD during the test reported in Fig. 6.

Fig. 9. Cars presented at the World Energy Council (Montréal, Sept. 2010), equipped with the battery C-LFP/LTO built with the same cells as described in the present work. Charging time is reduced to 5 min with three levels charger in parallel (500 V, 125 A).

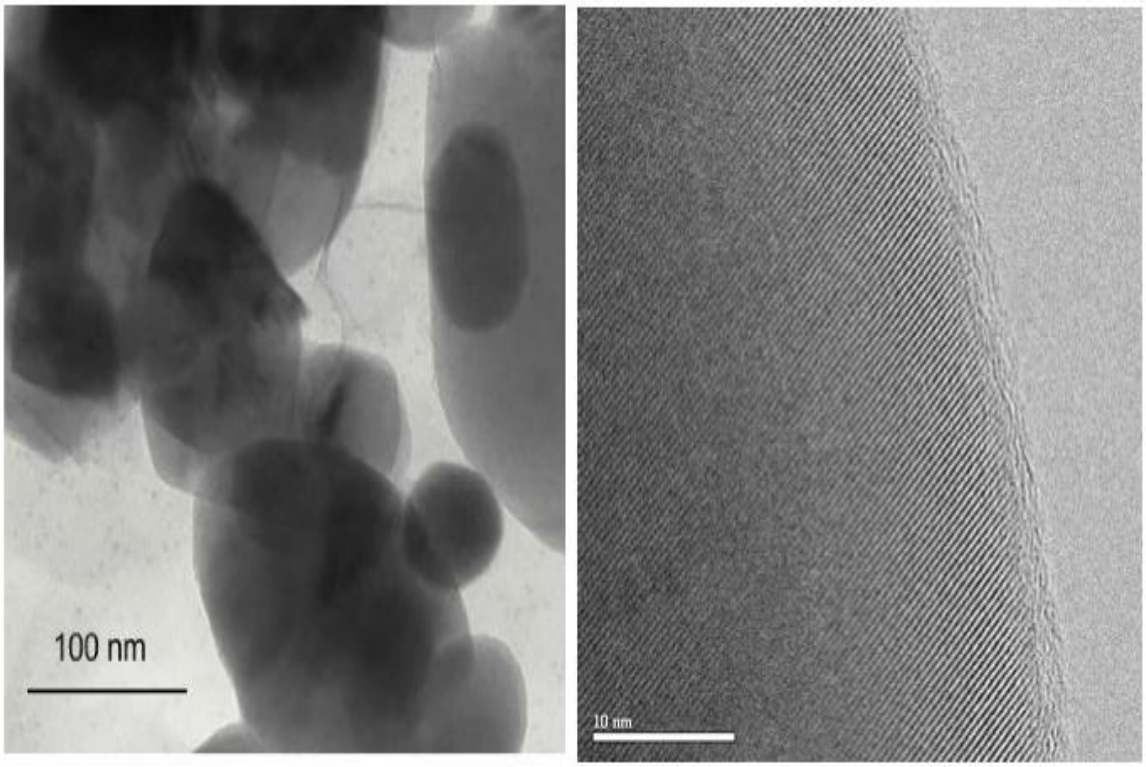

Figure 1.

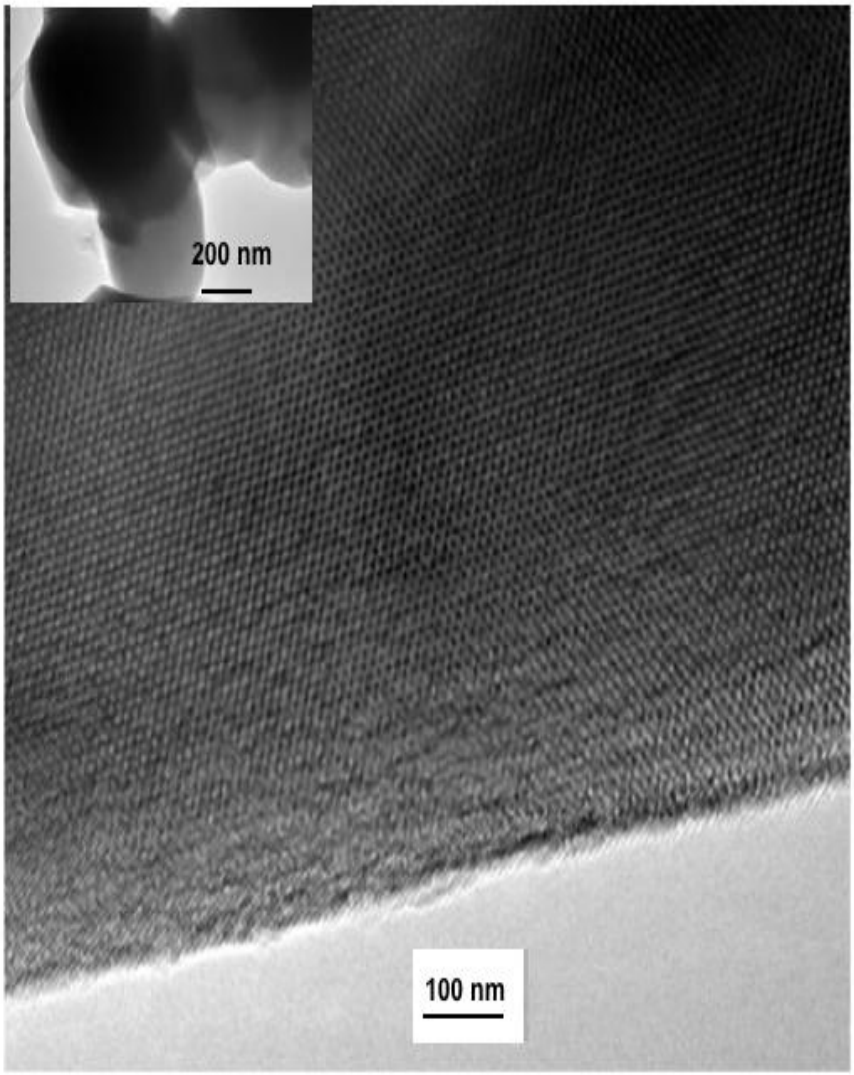

Figure 2.

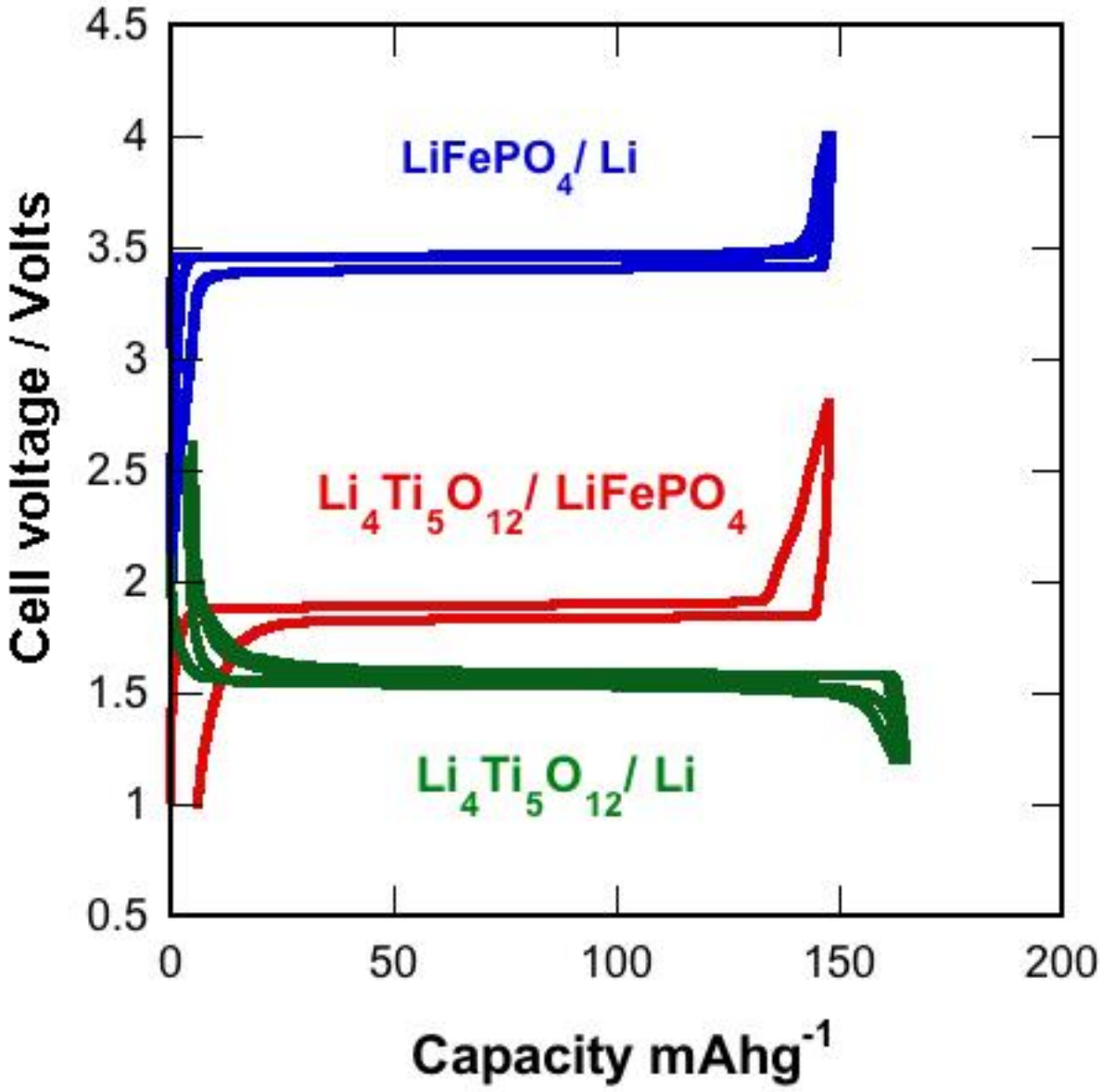

Figure 3.

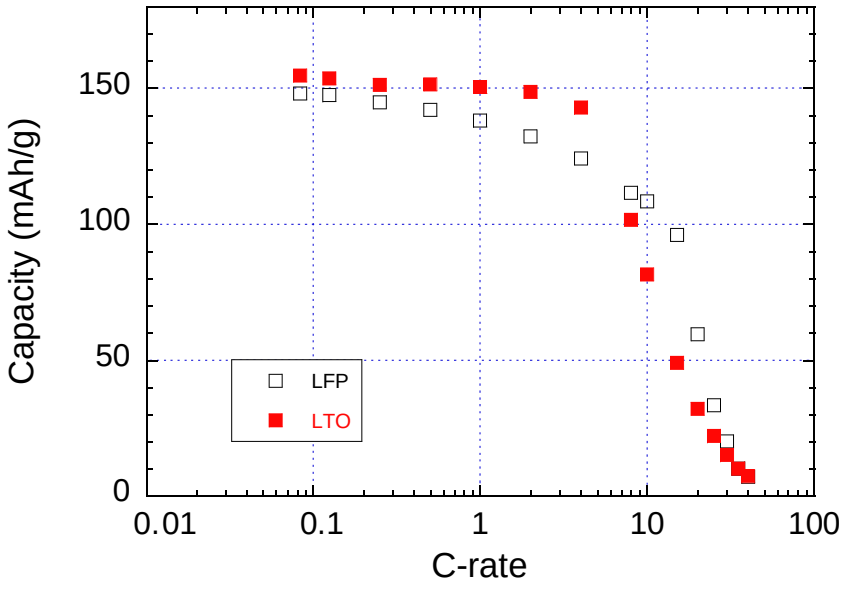

Figure 4.

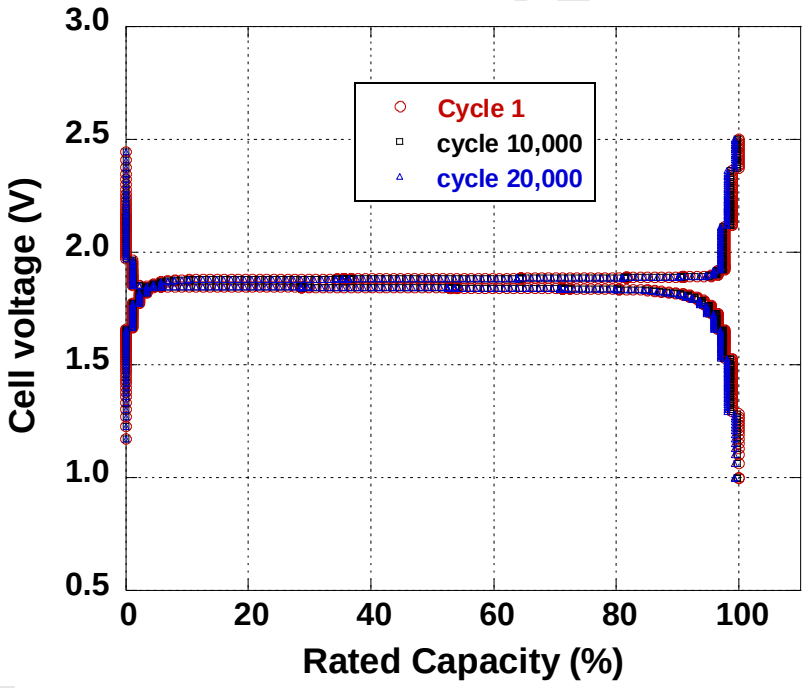

Figure 5.

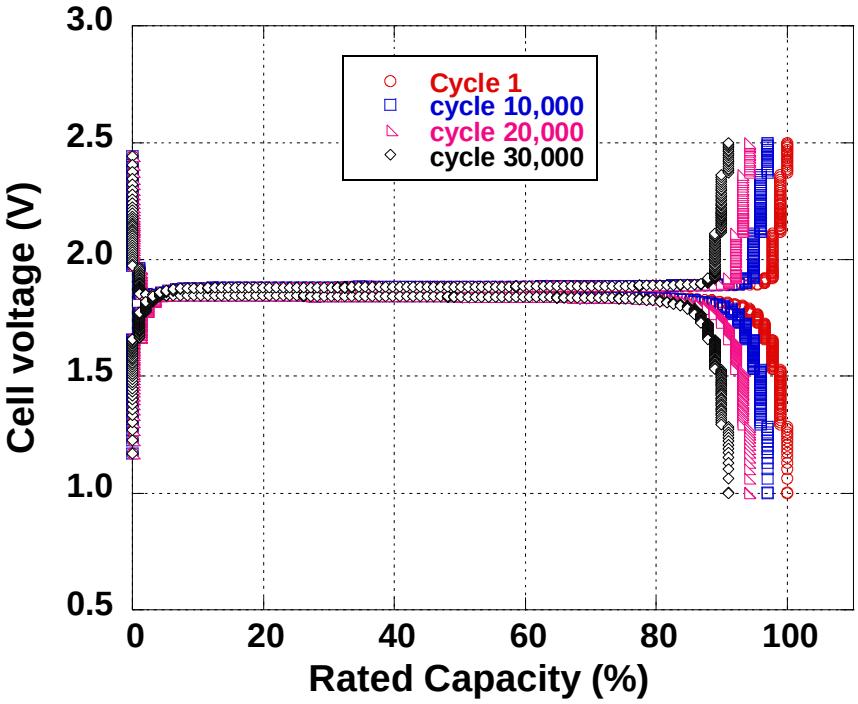

Figure 6.

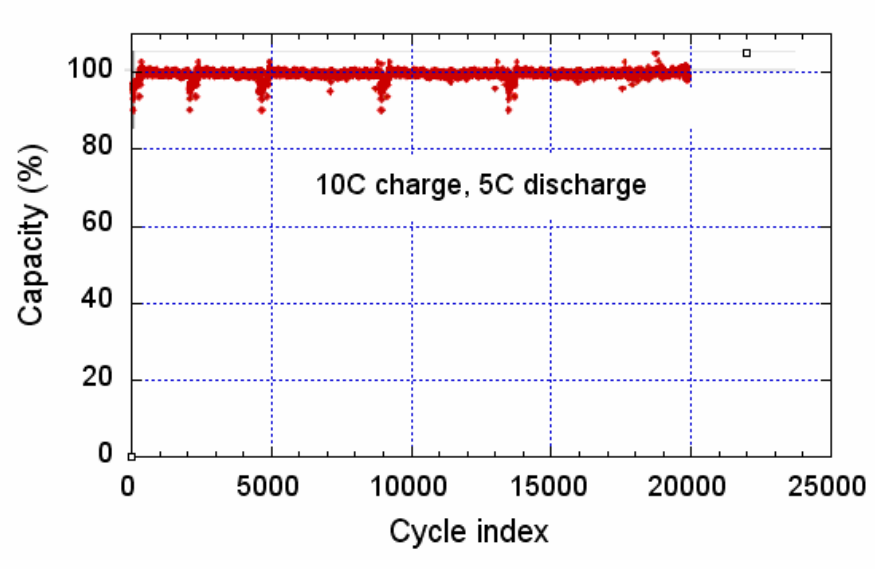

Figure 7.

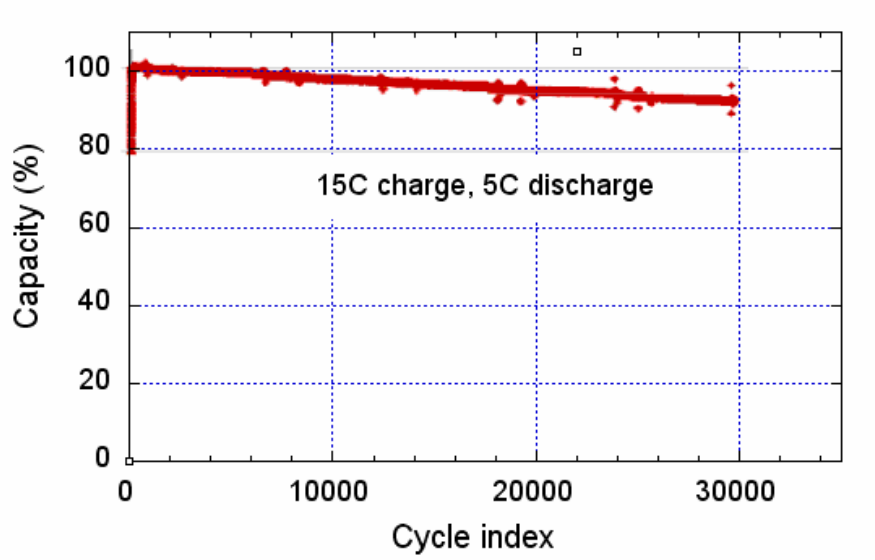

Figure 8.

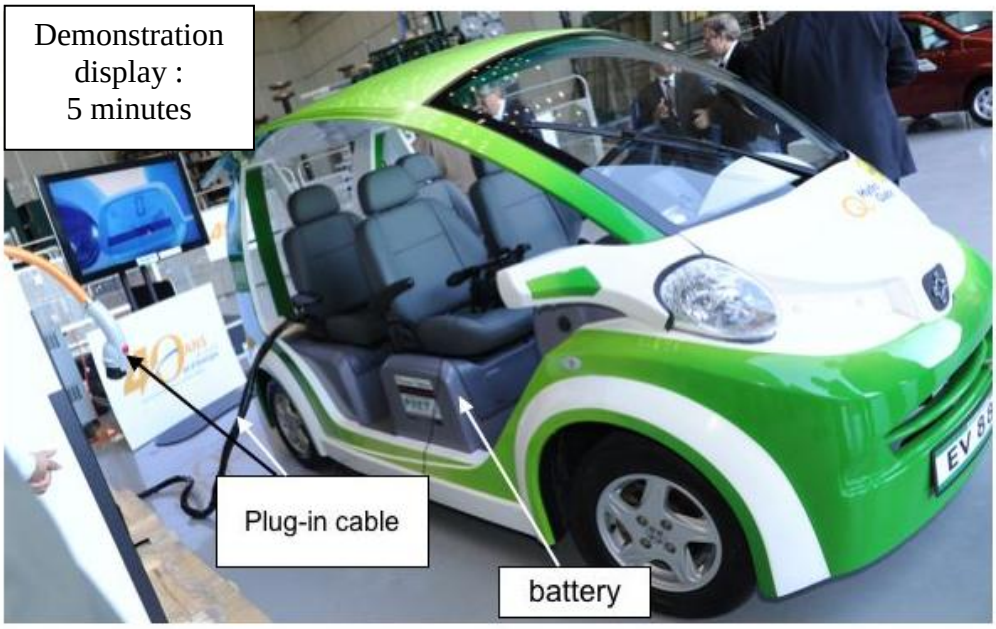

Figure 9.